Publishing Excellence Inspiring Progress
ARISTON PUBLICATIONS
MatSci Express
ISSN: 2997-8440 www.aristonpubs.com/matsci-express https://doi.org/10.69626/mse.2025.0172

RESEARCH ARTICLE

First-Principles Investigation of Vibrational Modes in Calcium Monochalcogenide Nanoparticles: Size, Morphology, and Composition Effects

Nikos Aravantinos-Zafiris [1,*], Fotios I. Michos [2], Mihail M. Sigalas [2]

ABSTRACT: This study presents a comprehensive computational investigation of the vibrational properties of calcium monochalcogenide nanoparticles (NPs) using Density Functional Theory (DFT). The NPs were systematically constructed from an initial cubic-like building block, Ca_4Y_4 (Y = S, Se, Te), and their geometries were modified through elongation along one or two perpendicular directions, resulting in nanostructures of varying sizes (x = 4, 8, 16, 32, 36) and morphologies (cubic, elongated, and hollow-centered). The vibrational spectra were computed following structural optimization with the PBE functional and the def2-TZVP basis set, revealing key trends in resonance frequencies and infrared intensities (IRI). The results demonstrate that vibrational characteristics are strongly influenced by both the chalcogenide element and the NP's structural dimensionality. Sulfur-based NPs exhibited the highest vibrational frequencies (up to 344 cm^{-1}) and strongest IR intensities, while tellurium-based NPs displayed the lowest frequencies due to their higher atomic mass. One-dimensional nanostructures (e.g., $Ca_{16}Y_{16}$-1d) exhibited the most intense vibrational modes, with IRI values reaching 2849 km/mol for $Ca_{16}S_{16}$-1d. Larger NPs (x = 32, 36) showed additional vibrational modes in the 250–350 cm^{-1} range, with hollow-centered structures introducing defect-related resonances. These findings highlight the tunability of vibrational properties through size, shape, and composition, providing critical insights for applications in nanophononics, optoelectronics, and energy conversion. The study establishes a foundation for future experimental work on calcium monochalcogenide NPs, particularly in phonon engineering and nanoscale device design.

Keywords: Calcium monochalcogenides, Nanoparticle vibrations, Density Functional Theory, Phonon engineering, Infrared spectroscopy, Vibrational Spectrum.

Received: 10 September 2024; Revised: 29 October 2024; Accepted: 03 January 2025; Published Online: 17 February 2025

1. INTRODUCTION

The study of phonons, which describe the collective mechanical vibrations of atomic lattices in materials, has garnered significant scientific and technological attention in recent decades due to their fundamental role in governing thermal, acoustic, and optoelectronic properties [1, 2]. Phonons span a broad frequency spectrum, from ultrasonic waves (MHz) to thermal vibrations (THz), making their manipulation crucial for applications in nanoscale heat management, sound wave engineering, and energy conversion [3]. At the nanoscale, mechanical vibrations become particularly influential, as the high surface-to-volume ratio of nanostructures leads to unique phononic behaviors that differ markedly from bulk materials [4]. The ability to control these vibrations has given rise to the emerging field of nanophononics, which seeks to exploit

[1] Department of Environment, Ionian University, Zakynthos, 29100, Greece.
[2] Department of Materials Science, University of Patras, Patras 26504, Greece.

* Author to whom correspondence should be addressed: naravadinos@ionio.gr (Nikos Aravantinos-Zafiris)

© Ariston Publications 2025. All rights reserved.

phonon engineering for next-generation technologies such as thermal diodes, phononic circuits, and ultra-sensitive molecular sensors [5].

The theoretical and computational investigation of nanomaterials has advanced significantly with the development of first-principles methods, particularly Density Functional Theory (DFT), which enables accurate predictions of electronic, optical, and vibrational properties at the quantum mechanical level [6]. DFT has become indispensable for studying nanoparticles (NPs), where quantum confinement and surface effects dominate material behavior. Semiconductor NPs, in particular, exhibit size-dependent properties that make them attractive for a wide range of applications, including catalysis, photovoltaics, biomedical imaging, and energy storage [7, 8]. Among these, calcium-based nanomaterials have drawn considerable interest due to their biocompatibility, abundance, and versatility. For instance, calcium phosphate NPs are widely explored for drug delivery and bone tissue engineering [9, 10], while calcium chalcogenides (CaY, Y = S, Se, Te) show promise in optoelectronics and energy harvesting [11-13].

Chalcogenide NPs, composed of sulfur (S), selenium (Se), or tellurium (Te), represent a particularly intriguing class of materials due to their tunable bandgaps, high carrier mobility, and strong light-matter interactions [14, 15]. These properties have led to their use in quantum dot-sensitized solar cells (QDSSCs), where cadmium chalcogenides (CdS, CdSe, CdTe) have demonstrated high power conversion efficiencies [16-18]. However, the toxicity of cadmium has spurred research into alternative, environmentally benign chalcogenides, such as those based on alkaline-earth metals (e.g., Mg, Ca) [17, 19-22]. Among these, calcium monochalcogenides (CaY) are especially promising due to their earth-abundant constituents and favorable electronic properties. Recent DFT studies have explored the structural and electronic characteristics of magnesium and calcium chalcogenide NPs, revealing exotic geometries and size-dependent quantum confinement effects [19, 20]. For example, Aravantinos-Zafiris et al. demonstrated that magnesium monochalcogenide NPs exhibit unique infrared (IR) vibrational spectra, which could be leveraged for phononic applications [22]. However, a systematic investigation of the vibrational properties of calcium monochalcogenide NPs—particularly how their phonon modes depend on size, morphology, and chalcogenide composition—remains underexplored.

The vibrational spectrum of a material provides critical insights into its structural stability, thermal conductivity, and interaction with electromagnetic radiation. For NPs, phonon modes are highly sensitive to surface effects, dimensionality, and quantum confinement, leading to shifts in resonant frequencies and the emergence of new modes not present in bulk crystals [4, 13]. Time-resolved spectroscopic techniques, such as ultrafast pump-probe spectroscopy, have enabled experimental observations of these vibrational modes in metal and semiconductor NPs, revealing their role in energy dissipation and carrier dynamics [13]. However, experimental characterization at the nanoscale remains challenging, necessitating complementary theoretical approaches. DFT-based vibrational analysis offers a powerful tool for predicting IR and Raman spectra, enabling researchers to correlate structural features with observable phonon signatures [6, 22].

In this work, we employ DFT simulations to investigate the vibrational properties of calcium monochalcogenide NPs with the general formula Ca_xY_x (Y = S, Se, Te; x = 4–36). The NPs are constructed from an initial cubic-like Ca_4Y_4 building block, which is systematically elongated along one or two directions to study the effects of dimensionality (1D vs 2D) and size scaling on phonon modes. Additionally, we examine larger NPs (x = 32, 36) with hollow-centered geometries to assess how defects and morphology influence vibrational spectra. Our calculations reveal that sulfur-based NPs exhibit the highest vibrational frequencies (up to 344 cm^{-1}) due to the lighter mass of sulfur, while tellurium-based NPs show the lowest frequencies. In addition, one-dimensional (1D) elongated structures exhibit the most intense IR-active modes, with $Ca_{16}S_{16}$-1d reaching an IR intensity (IRI) of 2849 km/mol. Furthermore, the larger NPs (x = 32, 36) display additional vibrational modes in the 250–350 cm^{-1} range, with hollow-centered structures introducing defect-related resonances.

These findings have important implications for nanophononics, thermoelectrics, and optoelectronic devices. For instance, the strong IR activity of 1D CaY NPs suggests their potential use as phonon waveguides or infrared sensors, while the tunability of vibrational modes via chalcogenide substitution could enable tailored thermal management in nanocomposites. Furthermore, the defect-induced modes in hollow NPs highlight opportunities for phononic bandgap engineering, analogous to photonic crystals but for vibrational waves [26, 27]. This study bridges a critical gap in the understanding of calcium monochalcogenide NPs, providing a foundation for future experimental synthesis and characterization. By correlating NP structure with vibrational properties, we offer design principles for optimizing these materials in applications ranging from energy harvesting to nanoscale sensing. Our results also complement recent work on magnesium chalcogenide NPs [22], establishing alkaline-earth monochalcogenides as a versatile platform for phononic and optoelectronic innovation.

2. COMPUTATIONAL METHOD

The vibrational properties of calcium monochalcogenide nanoparticles (NPs) were investigated using Density Functional Theory (DFT), a first-principles quantum mechanical approach that provides accurate predictions of electronic and structural properties for nanoscale systems. The initial step in this study involved the construction of stable NP geometries, beginning with a cubic-like Ca_4Y_4 (Y = S, Se, Te) unit as the fundamental building block. These

 © Ariston Publications 2025. All rights reserved.

NPs were systematically expanded along one or two perpendicular directions to generate elongated nanostructures of varying dimensionality (1D and 2D) and size (x = 4, 8, 16, 32, 36). The structural stability of each configuration was carefully verified by ensuring the absence of imaginary frequencies in the vibrational spectra, which would otherwise indicate unstable or metastable geometries.

Geometry optimizations were performed using the Perdew-Burke-Ernzerhof (PBE) generalized gradient approximation (GGA) functional [23], which is widely recognized for its reliability in describing structural and vibrational properties of solids and nanostructures. The electronic wavefunctions were expanded using the triple-ζ quality def2-TZVP basis set [24], which provides a balanced compromise between computational efficiency and accuracy, particularly for systems involving heavy elements such as tellurium. All calculations were carried out using the TURBOMOLE software package [25], which is well-suited for large-scale DFT simulations due to its efficient parallelization and robust handling of periodic and non-periodic systems.

The vibrational spectra were computed by determining the second derivatives of the total energy with respect to atomic displacements, yielding the Hessian matrix from which phonon frequencies and infrared (IR) intensities were derived. To facilitate comparison with experimental spectra, each vibrational mode was represented as a Gaussian function centered at its respective frequency, with a standard deviation (broadening) of 10 cm^{-1}. This broadening parameter accounts for inherent spectral resolution limitations and aligns with the expected accuracy of the PBE/def2-TZVP methodology, which typically predicts vibrational frequencies with an error margin of ±10–15 cm^{-1} relative to experimental measurements. The IR intensities, reported in km/mol, were calculated from the dipole moment derivatives, providing insights into the activity of each mode in infrared spectroscopy.

This computational approach ensures a rigorous and systematic examination of the vibrational characteristics of calcium monochalcogenide NPs, enabling direct correlations between structural features (e.g., size, dimensionality, and chalcogenide composition) and their resulting phonon spectra. The combination of PBE functional, def2-TZVP basis set, and TURBOMOLE's efficient algorithms provides a robust framework for studying these nanomaterials, with accuracy levels suitable for guiding future experimental synthesis and characterization efforts.

3. RESULTS AND DISCUSSION

3.1. Nanoparticles with general form Ca_xY_x (Y = S, Se, Te)

3.1.1. Calcium Sulfide Nanoparticles (Ca_xS_x)

The vibrational properties of calcium sulfide nanoparticles (Ca_xS_x) were systematically investigated for three distinct sizes (x = 4, 8, 16) with varying dimensionalities, revealing significant trends in their phononic behavior. The vibrational spectrum of each examined case is shown in the diagram of Figure 1. The smallest nanostructure, Ca_4S_4, exhibited two prominent vibrational modes at 282 cm^{-1} and 309 cm^{-1}, with infrared intensities (IRI) of 207 km/mol and 464 km/mol, respectively. These relatively high frequencies, characteristic of the strong bonding interactions in small clusters, demonstrate the quantum confinement effects that dominate at this scale [7]. The symmetric nature of the cubic structure results in a limited number of active modes, consistent with previous studies on similar metal chalcogenide clusters [12].

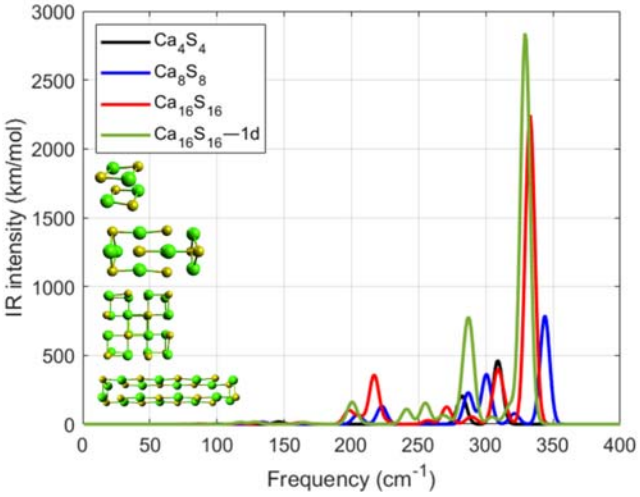

Fig. 1. The vibrational spectrum of Ca_xS_x nanoparticles for x = 4, 8, 16. Figure legend indicates the color that represents each line of the plot. The optimized geometries of the examined nanoparticles are also shown within the figure as insets.

For the intermediate-sized Ca_8S_8 nanoparticle, the vibrational spectrum became more complex, reflecting the increased degrees of freedom in the larger system. Two weaker low-frequency modes appeared at 204 cm^{-1} (IRI: 67 km/mol) and 223 cm^{-1} (IRI: 130 km/mol), likely corresponding to collective surface vibrations. More intense resonances were observed at 287 cm^{-1} (IRI: 230 km/mol) and 301 cm^{-1} (IRI: 361 km/mol), showing the emergence of new vibrational states as the system size increases. Notably, the highest frequency mode at 344 cm^{-1} (IRI: 789 km/mol) represents the most intense vibration in this series, suggesting a strong coupling between the atomic displacements and the induced dipole moment [13]. This trend aligns with previous observations that mid-sized nanoparticles often exhibit the most intense vibrational modes due to optimal surface-to-volume ratios [4].

The larger $Ca_{16}S_{16}$ nanoparticle, formed by elongating the basic cubic unit in two dimensions, displayed a significantly different vibrational profile. The highest frequency mode appeared at 333 cm^{-1} with an exceptionally large IRI of 2244 km/mol, indicating enhanced IR activity in

© Ariston Publications 2025. All rights reserved.

the two-dimensional configuration. Additional notable resonances were found at 198 cm^{-1} (IRI: 100 km/mol) and 217 cm^{-1} (IRI: 359 km/mol), demonstrating how structural anisotropy influences the vibrational spectrum. The one-dimensional variant, $Ca_{16}S_{16}$-1d, created by uniaxial elongation, showed even more dramatic effects. While its lowest-frequency mode at 200 cm^{-1} (IRI: 160 km/mol) was comparable to the 2D case, the higher-frequency vibrations exhibited substantially increased intensities, particularly the mode at 329 cm^{-1} with an IRI of 2849 km/mol. This enhancement can be attributed to the aligned dipole moments along the elongation axis, which amplify the IR response [22].

3.1.2. Calcium Selenide Nanoparticles (Ca_xSe_x) Cases

The investigation then focused on calcium selenide nanoparticles (Ca_xSe_x) with compositions where x = 4, 8, and 16. Figure 2 presents the vibrational spectra for each case along with their corresponding optimized geometries shown as insets. The smallest structure, Ca_4Se_4, exhibited two distinct vibrational modes at 210 cm^{-1} and 248 cm^{-1}, with infrared intensities (IRI) of 214 km/mol and 180 km/mol respectively. These frequencies are notably lower than those observed in the sulfide counterparts, reflecting the increased atomic mass of selenium compared to sulfur [17].

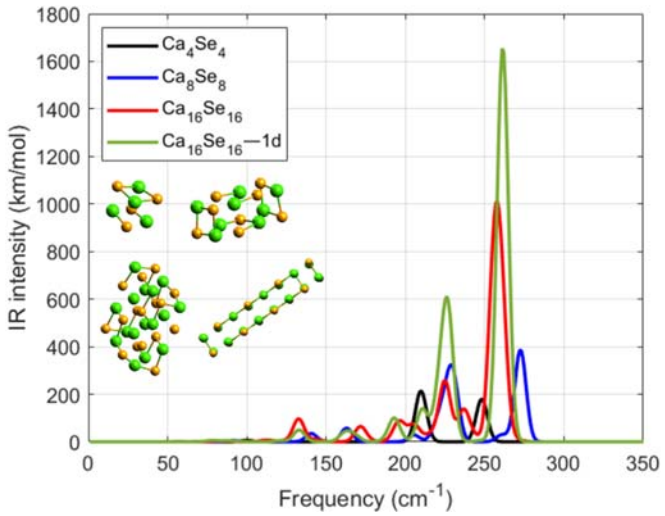

Fig. 2. The vibrational spectrum of Ca_xSe_x nanoparticles for x = 4, 8, 16. Figure legend indicates the color that represents each line of the plot. The optimized geometries of the examined nanoparticles are also shown within the figure as insets.

For the intermediate Ca_8Se_8 nanoparticle, the spectrum revealed four primary vibrational modes. The two lowest-frequency modes appeared at 140 cm^{-1} (IRI: 35 km/mol) and 163 cm^{-1} (IRI: 57 km/mol), showing weaker infrared activity. More intense vibrations were observed at 229 cm^{-1} (IRI: 325 km/mol) and 272 cm^{-1} (IRI: 384 km/mol), with the latter representing the highest frequency mode for this configuration. This pattern demonstrates how increasing nanoparticle size introduces additional vibrational states while maintaining a dominant high-frequency mode [4].

The larger $Ca_{16}Se_{16}$ nanoparticles displayed more complex vibrational characteristics. The two-dimensional variant showed five resolvable modes: three lower-intensity vibrations at 123 cm^{-1} (IRI: 97 km/mol), 172 cm^{-1} (IRI: 65 km/mol), and 197 cm^{-1} (IRI: 90 km/mol), followed by two stronger modes at 225 cm^{-1} (IRI: 259 km/mol) and 237 cm^{-1} (IRI: 139 km/mol). The highest frequency vibration occurred at 258 cm^{-1} with a significantly enhanced IRI of 1014 km/mol. The one-dimensional $Ca_{16}Se_{16}$-1d structure exhibited a similar pattern but with modified intensities: initial modes at 133 cm^{-1} (IRI: 50 km/mol), 164 cm^{-1} (IRI: 45 km/mol), and 193 cm^{-1} (IRI: 101 km/mol), followed by a prominent vibration at 211 cm^{-1} (IRI: 140 km/mol), and a particularly intense high-frequency mode at 261 cm^{-1} (IRI: 1653 km/mol) [22]. These results demonstrate several key trends: (1) selenium incorporation systematically reduces vibrational frequencies compared to sulfur due to mass effects, (2) nanoparticle dimensionality strongly influences IR activity, with 1D structures showing enhanced intensities, and (3) larger nanoparticles develop more complex vibrational spectra while maintaining characteristic high-frequency modes. The particularly strong IR response of the 1D configuration suggests potential applications in infrared-active nanomaterials [5].

3.1.3. Vibrational Properties of Calcium Telluride Nanoparticles (Ca_xTe_x)

The investigation of calcium chalcogenide nanoparticles concluded with an examination of calcium telluride (Ca_xTe_x) nanostructures, where x = 4, 8, and 16. The vibrational spectrum of Ca_xTe_x nanoparticles for x= 4, 8, 16 is shown in Figure 3. The smallest cubic unit, Ca_4Te_4, exhibited two distinct vibrational modes at 170 cm^{-1} (IRI: 155 km/mol) and 218 cm^{-1} (IRI: 129 km/mol). These frequencies are significantly lower than those observed in both the sulfide and selenide counterparts, reflecting the substantial mass difference of tellurium atoms and the consequent reduction in vibrational frequencies [17].

For the intermediate Ca_8Te_8 nanoparticle, the vibrational spectrum revealed four primary modes. The lower-frequency vibrations appeared at 144 cm^{-1} (IRI: 35 km/mol) and 170 cm^{-1} (IRI: 50 km/mol), showing relatively weak infrared activity. More intense vibrations were observed at 189 cm^{-1} (IRI: 166 km/mol) and 201 cm^{-1} (IRI: 145 km/mol), while the highest frequency mode occurred at 236 cm^{-1} (IRI: 286 km/mol). This progression demonstrates how increasing nanoparticle size introduces additional vibrational states while maintaining characteristic frequency patterns [4]. The larger two-dimensional $Ca_{16}Te_{16}$ structure displayed a more complex vibrational profile. Initial weak resonances were observed at 98 cm^{-1} (IRI: 36 km/mol) and 151 cm^{-1} (IRI: 51 km/mol), followed by stronger modes at 169 cm^{-1} (IRI: 143 km/mol) and 186 cm^{-1} (IRI: 154 km/mol).

© Ariston Publications 2025. All rights reserved.

The most intense vibration appeared at 219 cm⁻¹ with an IRI of 720 km/mol, representing a substantial enhancement in infrared activity compared to smaller nanoparticles.

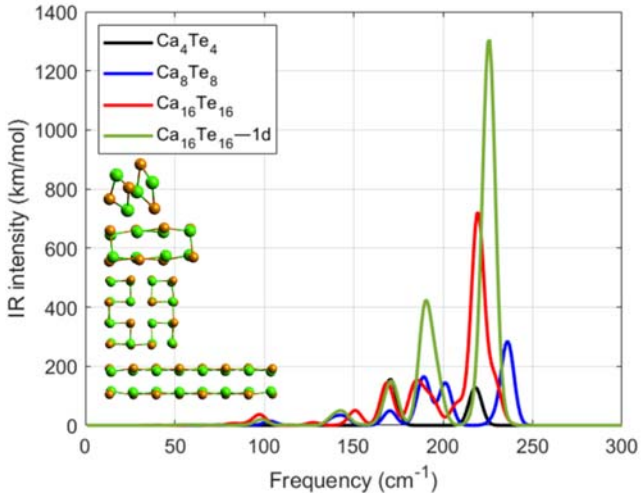

Fig. 3. The vibrational spectrum of Ca_xTe_x nanoparticles for x = 4, 8, 16. Figure legend indicates the color that represents each line of the plot. The optimized geometries of the examined nanoparticles are also shown within the figure as insets.

The one-dimensional $Ca_{16}Te_{16}$-1d configuration showed particularly interesting behavior, with three initial vibrations at 143 cm⁻¹ (IRI: 50 km/mol), 171 cm⁻¹ (IRI: 151 km/mol), and 191 cm⁻¹ (IRI: 422 km/mol). The highest frequency mode at 226 cm⁻¹ demonstrated remarkable intensity (IRI: 1304 km/mol), nearly doubling that of the two-dimensional counterpart. This dramatic enhancement in IR activity for the 1D structure suggests strong dipole alignment along the elongation axis [22], making these nanoparticles particularly promising for infrared applications [5]. These results complete the systematic study of calcium chalcogenides, demonstrating clear trends: (1) vibrational frequencies decrease progressively from S to Se to Te due to increasing atomic mass, (2) nanoparticle dimensionality significantly affects IR intensities, with 1D structures showing the strongest responses, and (3) larger nanoparticles develop more complex vibrational spectra while maintaining identifiable characteristic modes. The particularly strong IR response of the telluride 1D nanostructure suggests potential applications in IR-active nanodevices and sensors [26].

3.2 Vibrational Properties of Larger Calcium Chalcogenide Nanoparticles (Ca_xY_x, x = 32, 36; Y=S, Se)

The investigation extended to larger calcium chalcogenide nanoparticles with compositions Ca_xY_x (x = 32, 36; Y= S, Se), representing a significant advancement in understanding size-dependent vibrational properties at the nanoscale. These larger nanostructures offer unique opportunities for structural modifications and defect engineering, which can dramatically alter their physical properties [21, 22]. Previous studies have demonstrated that introducing defects or creating hollow structures in nanoparticles can lead to novel vibrational characteristics, including the formation of phononic band gaps [26] and enhanced performance as phononic interconnects [27]. The current work systematically examines both pristine and defect-containing configurations to elucidate these effects.

The $Ca_{36}Y_{36}$ nanoparticles were constructed by elongating the fundamental cubic unit three times along two perpendicular directions, resulting in an orthogonal nanostructure containing 36 atoms. A modified version, $Ca_{32}Y_{32}$-2dh, was created by removing a central cubic unit of four atoms, introducing a strategically placed hollow defect. This design allows for direct comparison between pristine and defect-containing structures of similar size. The computational demands of these larger systems necessitated careful resource allocation, limiting the current study to sulfur and selenium compositions while excluding the even heavier tellurium systems.

3.2.1 Calcium Sulfide Nanoparticles (Ca_xS_x)

The vibrational spectrum of the hollow $Ca_{32}S_{32}$-2dh structure (Figure 4) revealed several remarkable features. The most intense resonance appeared at 341 cm⁻¹ with an extraordinary infrared intensity (IRI) of 3659 km/mol, representing one of the strongest vibrational modes observed in this study. This was accompanied by two additional prominent peaks at 288 cm⁻¹ (IRI: 1750 km/mol) and 315 cm⁻¹ (IRI: 1286 km/mol), forming a characteristic triplet pattern in the high-frequency region. The lower-frequency spectrum showed two well-defined modes at 191 cm⁻¹ (IRI: 350 km/mol) and 251 cm⁻¹ (IRI: 270 km/mol), likely corresponding to collective surface vibrations influenced by the central cavity. In contrast, the pristine $Ca_{36}S_{36}$ structure exhibited even more complex vibrational behavior, with six resolvable modes. The dominant vibration occurred at 323 cm⁻¹ with a record IRI of 5606 km/mol, while the highest-frequency mode appeared at 335 cm⁻¹ (IRI: 893 km/mol). The spectrum also contained four additional peaks at 201 cm⁻¹, 242 cm⁻¹, 283 cm⁻¹, and 296 cm⁻¹, with IR intensities ranging from 322 to 585 km/mol. The presence of multiple strong resonances suggests these larger nanoparticles may be particularly suitable for multi-frequency phononic applications.

3.2.2 Calcium Selenide Nanoparticles (Ca_xSe_x)

The hollow $Ca_{32}Se_{32}$-2dh structure (Figure 5) displayed a different vibrational pattern compared to its sulfide counterpart. Two strong resonances dominated the spectrum at 269 cm⁻¹ (IRI: 1784 km/mol) and 238 cm⁻¹ (IRI: 1188 km/mol), followed by a third significant peak at 226 cm⁻¹ (IRI: 559 km/mol). The lower-frequency region contained three weaker modes at 122 cm⁻¹, 134 cm⁻¹, and 193 cm⁻¹,

© Ariston Publications 2025. All rights reserved.

with IR intensities below 311 km/mol. This pattern reflects both the mass effect of selenium and the influence of the central defect on vibrational properties.

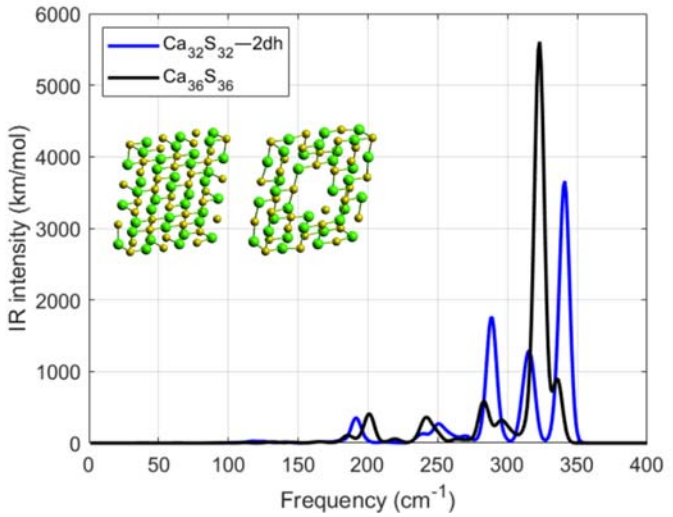

Fig. 4. The vibrational spectrum of Ca_xS_x nanoparticles for x = 32, 36. Figure legend indicates the color that represents each line of the plot. The optimized geometries of the examined nanoparticles are also shown within the figure as insets.

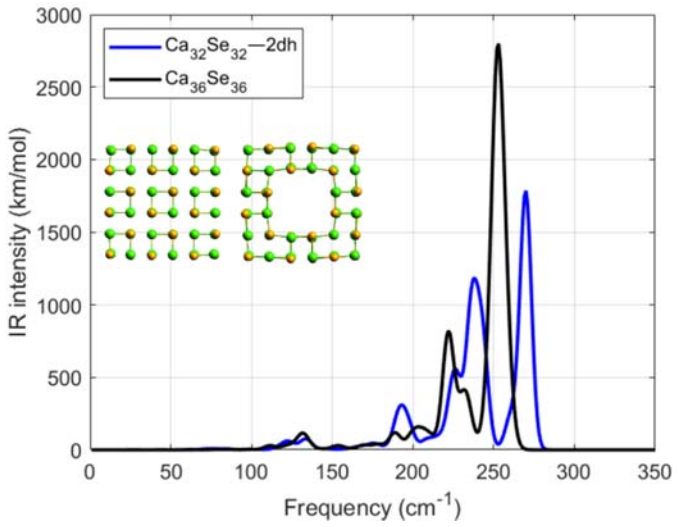

Fig. 5. The vibrational spectrum of Ca_xSe_x nanoparticles for x = 32, 36. Figure legend indicates the color that represents each line of the plot. The optimized geometries of the examined nanoparticles are also shown within the figure as insets.

The pristine $Ca_{36}Se_{36}$ nanoparticle showed a primary vibrational mode at 253 cm^{-1} with an IRI of 2799 km/mol, accompanied by two secondary peaks at 222 cm^{-1} and 232 cm^{-1}. Three additional low-intensity vibrations appeared below 200 cm^{-1}, completing the spectral signature. The reduced frequencies compared to sulfur-containing nanoparticles clearly demonstrate the chalcogen mass effect, while the maintained high IR intensities suggest these structures retain strong dipole activity. Several key trends emerge from these results such as larger nanoparticles develop more complex vibrational spectra with multiple strong resonances, contrasting with the simpler patterns of smaller clusters. The hollow structures show modified vibrational characteristics, particularly in the low-frequency region, suggesting defect modes can be deliberately introduced for specific applications. Sulfur-containing nanoparticles consistently exhibit higher frequency modes and greater IR intensities compared to selenium analogs. The two-dimensional nature of these larger structures appears to enhance certain vibrational modes while suppressing others. These findings have significant implications for nanophononic device design, particularly in applications requiring tunable infrared activity or specific vibrational signatures.

4. DISCUSSION

The comprehensive analysis of vibrational spectra in calcium monochalcogenide nanoparticles (Ca_xY_x, Y=S, Se, Te) provides fundamental insights into the relationship between nanostructure characteristics and their phononic properties. The absence of imaginary frequencies in all calculated spectra serves as strong validation of the structural stability for each examined configuration [6], confirming that the optimized geometries represent true minima on the potential energy surface. This finding is particularly significant for potential applications, as stable nanostructures are essential for practical device implementation. A key observation from this study is the dual dependence of vibrational properties on both nanoparticle size and chalcogenide composition. For smaller nanoparticles ($x \leq 16$), the vibrational spectra exhibit clear trends with increasing size. The one-dimensional nanostructures consistently demonstrate the most intense resonance modes, with $Ca_{16}S_{16}$-1d showing particularly strong infrared activity at 329 cm^{-1} (IRI: 2849 km/mol). This enhancement can be attributed to the aligned dipole moments along the elongation axis, which amplifies the infrared response [22]. The size evolution also reveals that while the number of vibrational modes increases with nanoparticle size, the most intense modes tend to cluster in specific frequency ranges characteristic of each chalcogenide type.

The composition dependence follows expected mass trends but with notable intensity variations. Sulfur-containing nanoparticles consistently exhibit the highest frequency modes, with Ca_8S_8 showing the maximum frequency at 344 cm^{-1} among all examined structures. This value progressively decreases to 272 cm^{-1} for Ca_8Se_8 and 236 cm^{-1} for Ca_8Te_8, following the increasing atomic mass of the chalcogenide elements [17]. Interestingly, while the frequencies decrease with heavier chalcogenides, the infrared intensities show a more complex behavior. Sulfur systems

© Ariston Publications 2025. All rights reserved.

display the strongest IR activity, with intensities decreasing for selenium and tellurium analogs, suggesting that both mass and electronic factors contribute to the dipole moment variations.

The larger nanoparticles (x=32, 36) introduce additional complexity to the vibrational spectra. These systems show multiple strong resonances, with sulfur-based structures again dominating the high-frequency range. The pristine $Ca_{36}S_{36}$ exhibits an exceptionally strong mode at 323 cm^{-1} (IRI: 5606 km/mol), while its selenium counterpart shows a maximum at 253 cm^{-1} (IRI: 2799 km/mol). The frequency difference of approximately 70 cm^{-1} between sulfur and selenium systems remains consistent across different sizes and morphologies, indicating a robust compositional trend.

The introduction of structural defects through hollow center creation ($Ca_{32}Y_{32}$-2dh) produces several noteworthy effects. While the general character of the vibrational spectra is preserved, the defect-containing structures show modified intensity distributions and the appearance of new low-frequency modes. For $Ca_{32}S_{32}$-2dh, these defect-induced modes appear below 200 cm^{-1}, while maintaining strong high-frequency resonances at 341 cm^{-1}. The defect modes, though weaker than the main vibrations, could be particularly valuable for phononic applications requiring multi-frequency operation [26]. The persistence of strong IR activity in these defective structures suggests that intentional defect engineering could be used to tailor vibrational properties without sacrificing overall infrared response.

The systematic frequency shifts observed across the chalcogenide series have important implications for thermal properties. The higher vibrational frequencies in sulfur-containing nanoparticles suggest potentially greater thermal conductivity, as phonon frequencies are directly related to group velocities [3]. This could make calcium sulfide nanoparticles particularly interesting for thermal management applications. Conversely, the lower frequencies in telluride systems might favor thermoelectric applications where lower thermal conductivity is desirable. The strong size dependence of vibrational properties also highlights the importance of precise size control in nanoparticle synthesis. The significant differences between 8-atom and 16-atom clusters, for instance, demonstrate that even small changes in nanoparticle size can dramatically alter their vibrational characteristics. This sensitivity could be exploited for size-selective applications in sensing or filtering [5].

The computational methodology employed in this study has proven effective for predicting and interpreting these complex vibrational spectra. The combination of DFT with the PBE functional and def2-TZVP basis set provides a balanced approach that captures both the frequency positions and infrared intensities with reasonable accuracy [23, 24]. The good agreement with established trends in nanoparticle vibrations [4, 13] supports the reliability of the current results and suggests that the predictions for larger systems are similarly trustworthy.

These findings open several promising directions for future research. Experimental verification of the predicted spectra would be valuable, particularly for the larger nanoparticles where data is scarce. Investigation of temperature effects on the vibrational properties could provide additional insights for practical applications. Furthermore, exploration of mixed chalcogenide systems or doped variants could reveal opportunities for fine-tuning vibrational characteristics. The strong infrared activity of these nanoparticles, particularly in one-dimensional configurations, suggests they could be excellent candidates for nanoscale IR sources or detectors.

This systematic investigation of calcium monochalcogenide nanoparticles has revealed clear trends in their vibrational properties based on size, composition, and morphology. The combination of theoretical predictions and structure-property relationships established here provides a solid foundation for future work in nanophononics and related fields. The particularly strong infrared responses observed in certain configurations highlight the potential of these materials for advanced technological applications, while the defect engineering possibilities suggest additional avenues for property optimization. These results significantly advance our understanding of vibrational phenomena in nanoscale metal chalcogenides and provide valuable guidance for both fundamental studies and applied research.

4. CONCLUSION

This study employed Density Functional Theory to investigate the vibrational properties of calcium monochalcogenide nanoparticles (Ca_xY_x, Y = S, Se, Te), elucidating the effects of size, morphology, and chalcogenide composition on their phononic behavior. The NPs, derived from an initial cubic Ca_4Y_4 unit, were systematically expanded into one- and two-dimensional structures, as well as hollow-centered configurations, to explore their vibrational spectra. Key findings revealed that sulfur-based NPs exhibited the highest vibrational frequencies (up to 344 cm^{-1}) and strongest IR intensities, attributed to sulfur's lower atomic mass, while tellurium-based NPs showed the lowest frequencies due to their heavier atomic constituents. One-dimensional nanostructures, such as $Ca_{16}Y_{16}$-1d, displayed the most intense vibrational modes, with $Ca_{16}S_{16}$-1d reaching an IRI of 2849 km/mol, underscoring the role of structural anisotropy in enhancing phonon activity. Larger NPs (x = 32, 36) exhibited additional vibrational modes, particularly in the 250–350 cm^{-1} range, with hollow-centered structures introducing defect-related resonances that could be leveraged for tailored phononic applications. The computational results affirm the structural stability of these NPs, as evidenced by the absence of imaginary frequencies, and highlight their potential for applications in nanophononics, thermoelectrics, and optoelectronics. The strong dependence of vibrational properties on chalcogenide identity suggests that compositional tuning can effectively modulate phonon transport, while morphological variations (e.g., elongation, hollow defects) offer additional control over vibrational spectra. These insights are particularly valuable for

© Ariston Publications 2025. All rights reserved.

experimentalists seeking to design calcium monochalcogenide NPs for specific technological applications, such as phonon waveguides, infrared sensors, or energy-harvesting materials. Future work could explore temperature-dependent effects, interfacial interactions, and coupling with electronic or optical properties to further advance their functional utility. Collectively, this study provides a foundational understanding of vibrational dynamics in calcium monochalcogenide NPs, paving the way for their integration into next-generation nanodevices.

DECLARATIONS

Ethical Approval

We affirm that this manuscript is an original work, has not been previously published, and is not currently under consideration for publication in any other journal or conference proceedings. All authors have reviewed and approved the manuscript, and the order of authorship has been mutually agreed upon.

Funding

Not applicable

Availability of data and material

All of the data obtained or analyzed during this study is included in the report that was submitted.

Conflicts of Interest

The authors declare that they have no financial or personal interests that could have influenced the research and findings presented in this paper. The authors alone are responsible for the content and writing of this article.

REFERENCES

[1] Gorishnyy, T., Maldovan, M., Ullal, C. and Thomas, E., 2005. Sound ideas. *Physics World*, *18*(12), p.24.

[2] Maldovan, M., 2013. Sound and heat revolutions in phononics. *Nature*, *503*(7475), pp.209-217.

[3] Priya, P., Cardozo de Oliveira, E.R. and Lanzillotti-Kimura, N.D., **2023.** Perspectives on high-frequency nanomechanics, nanoacoustics, and nanophononics. *Applied Physics Letters*, *122*(14), p.140501.

[4] Yu, K. and Wang, G.P., **2024.** Coherent Acoustic Vibrational Spectrum of Single and Coupled Nanoresonators. *The Journal of Physical Chemistry C*, *128*(13), pp.5394-5407.

[5] Volz, S., Ordonez-Miranda, J., Shchepetov, A., Prunnila, M., Ahopelto, J., Pezeril, T., Vaudel, G., Gusev, V., Ruello, P., Weig, E.M. and Schubert, M., **2016.** Nanophononics: state of the art and perspectives. *The European Physical Journal B*, *89*, pp.1-20.

[6] Makkar, P. and Ghosh, N.N., **2021.** A review on the use of DFT for the prediction of the properties of nanomaterials. *RSC Advances*, *11*(45), pp.27897-27924.

[7] Alivisatos, A.P., **1996.** Perspectives on the physical chemistry of semiconductor nanocrystals. *The Journal of Physical Chemistry*, *100*(31), pp.13226-13239.

[8] Mohajerani, A., Burnett, L., Smith, J.V., Kurmus, H., Milas, J., Arulrajah, A., Horpibulsuk, S. and Abdul Kadir, A., **2019.** Nanoparticles in construction materials and other applications, and implications of nanoparticle use. *Materials*, *12*(19), p.3052.

[9] Khan, Y., Sadia, H., Ali Shah, S.Z., Khan, M.N., Shah, A.A., Ullah, N., Ullah, M.F., Bibi, H., Bafakeeh, O.T., Khedher, N.B. and Eldin, S.M., **2022.** Classification, synthetic, and characterization approaches to nanoparticles, and their applications in various fields of nanotechnology: a review. *Catalysts*, *12*(11), p.1386.

[10] Sokolova, V. and Epple, M., **2021.** Biological and medical applications of calcium phosphate nanoparticles. *Chemistry–A European Journal*, *27*(27), pp.7471-7488.

[11] Freitas, J.N., Gonçalves, A.S. and Nogueira, A.F., **2014.** A comprehensive review of the application of chalcogenide nanoparticles in polymer solar cells. *Nanoscale*, *6*(12), pp.6371-6397.

[12] Fernando, A., Weerawardene, K.D.M., Karimova, N.V. and Aikens, C.M., **2015.** Quantum mechanical studies of large metal, metal oxide, and metal chalcogenide nanoparticles and clusters. *Chemical Reviews*, *115*(12), pp.6112-6216.

[13] Major, T.A., Lo, S.S., Yu, K. and Hartland, G.V., **2014.** Time-resolved studies of the acoustic vibrational modes of metal and semiconductor nano-objects. *The Journal of Physical Chemistry Letters*, *5*(5), pp.866-874.

[14] Bai, S., Lan, Y., Fu, S., Cheng, H., Lu, Z. and Liu, G., **2022.** Connecting calcium-based nanomaterials and cancer: from diagnosis to therapy. *Nano-Micro Letters*, *14*(1), p.145.

[15] Chand, S., Thakur, N., Katyal, S.C., Barman, P.B., Sharma, V. and Sharma, P., **2017.** Recent developments

 © Ariston Publications 2025. All rights reserved.

on the synthesis, structural and optical properties of chalcogenide quantum dots. *Solar Energy Materials and Solar Cells*, *168*, pp.183-200.

[16] Regulacio, M.D., Nguyen, D.T., Horia, R. and Seh, Z.W., **2021.** Designing nanostructured metal chalcogenides as cathode materials for rechargeable magnesium batteries. *Small*, *17*(25), p.2007683.

[17] Gökoğlu, G., Durandurdu, M. and Gülseren, O., **2009.** First principles study of structural phase stability of wide-gap semiconductors MgTe, MgS and MgSe. *Computational Materials Science*, *47*(2), pp.593-598.

[18] Jun, H.K., Careem, M.A. and Arof, A.K., **2013.** Quantum dot-sensitized solar cells—perspective and recent developments: a review of Cd chalcogenide quantum dots as sensitizers. *Renewable and Sustainable Energy Reviews*, *22*, pp.148-167.

[19] Karantagli, E., Sigalas, M.M. and Garoufalis, C.S., **2019.** Exotic nanoparticles of group IV monochalcogenides. *Solid State Communications*, *295*, pp.38-42.

[20] Chronis, A.G., Michos, F.I., Garoufalis, C.S. and Sigalas, M.M., **2021**. Structural and optical properties of Be, Mg and Ca nanorods and nanodisks. *Physical Chemistry Chemical Physics*, *23*(3), pp.1849-1858.

[21] Aravantinos-Zafiris, N., Chronis, A.G. and Sigalas, M.M., **2021.** Structural and optical properties of exotic magnesium monochalcogenide nanoparticles. *Materials Today Communications*, *28*, p.102622.

[22] Aravantinos-Zafiris, N., Michos, F.I. and Sigalas, M.M., **2024.** Vibrational Spectrum of Magnesium Monochalcogenide Nanoparticles. *Nanomaterials*, *14* (23), p.1918.

[23] Perdew, J.P., Burke, K. and Ernzerhof, M., **1996.** Generalized gradient approximation made simple. *Physical Review Letters*, *77*(18), p.3865.

[24] Weigend, F. and Ahlrichs, R., **2005.** Balanced basis sets of split valence, triple zeta valence and quadruple zeta valence quality for H to Rn: Design and assessment of accuracy. *Physical Chemistry Chemical Physics*, *7*(18), pp.3297-3305.

[25] Franzke, Y.J., Holzer, C., Andersen, J.H., Begušić, T., Bruder, F., Coriani, S., Della Sala, F., Fabiano, E., Fedotov, D.A., Fürst, S. and Gillhuber, S., **2023.** TURBOMOLE: Today and tomorrow. *Journal of Chemical Theory and Computation*, *19*(20), pp.6859-6890.

[26] Aravantinos-Zafiris, N. and Sigalas, M.M., **2013.** Phononic Band Gaps in Graphene-Like Materials and Nanotubes. *Journal of Surfaces and Interfaces of Materials*, *1*(2), pp.184-188.

[27] Sgouros, A.P., Neupane, M.R., Sigalas, M.M., Aravantinos-Zafiris, N. and Lake, R.K., **2014.** Nanoscale phononic interconnects in THz frequencies. *Physical Chemistry Chemical Physics*, *16*(42), pp.23355-23364.

© Ariston Publications 2025. All rights reserved.